Available online at www.sciencedirect.com

ScienceDirect

Procedia Structural Integrity 47 (2023) 43–47

Structural Integrity Procedia

www.elsevier.com/locate/procedia

27th International Conference on Fracture and Structural Integrity (IGF27)

Parametric failure analysis of metal-based composites

Gabriella Bolzon*, Marco Talassi

Department of Civil and Environmental Engineering, Politecnico di Milano, piazza Leonardo da Vinci 32, 20133 Milano, Italy

Abstract

Metal-based composites can fail as a consequence of the growth and coalescence of micro-voids introduced with the manufacturing process. These detrimental phenomena influence the overall performance of the material to different extents since the macroscopic characteristics depend on both the local constitutive properties and geometry patterns, which promote various stress concentration and strain localization effects. The understanding of the different situations that arise in this context is often assisted by numerical simulations based on the GNT constitutive model, first proposed by Gurson (1977) and then refined by Needleman and Tvergaard (1984). However, exploring the influence of the most relevant material parameters on the composite response can be excessively time consuming. Therefore, traditional simulations based on non-linear finite element methods can be replaced by surrogate analytical approximations, which do not involve large computing costs but exhibit accuracy and sensitivity to the model parameters consistent with the practical applications. Some examples are presented in this contribution.

Keywords: Metal-based composites; failure; parametric studies; surrogate models.

1. Introduction

The performances of structural components made of composites can be optimized by including the micromechanical details and the local material properties in the design phase. The best configuration can then be obtained with the aid of parametric studies carried out on (often, numerical) models, which also provide the overall material strength and identify the likely failure mode(s).

* Corresponding author. Tel.: +39-02-2399-4319; fax: +30-02-2399-4330.
E-mail address: gabriella.bolzon@polimi.it

10.1016/j.prostr.2023.06.039

Metal-based composites fail by two main mechanisms, which consists in the separation of the interfaces between different constituents (Bolzon and Pitchai, 2017; Palizvan et al., 2020; Bolzon and Pitchai, 2022), and of the development of cracks in the matrix and/or the reinforcement (Bonora and Ruggiero, 2006). In metals, fracture is often driven by the growth and coalescence of micro-voids (Babout et al., 2001; Babout et al., 2004). These damaging processes are promoted by stress concentration effects that are pronounced in ceramic-reinforced metal-based composites due to the high difference in stiffness of the components; see, e.g. Bolzon and Pitchai (2017) and references therein.

The phenomenological constitutive law introduced by Gurson (1977) and refined by Needleman and Tvergaard (1984) (therefore, briefly named GNT) can describe the damage evolution in metals, leading to the formation of localized strain bands and, eventually, to material separation. These physical phenomena can be reproduced by usually expensive non-linear finite element (FE) analyses (Vaz et al., 2016).

The computing costs can be reduced in the case of long fiber composites, which are often characterized by a regular (at least, to some extent) arrangement of the reinforcement. Therefore, simulations can be limited to periodic representative volume elements. In fact, while strain localization is known to destroy symmetries and provide mesh sensitive results (Hild at al., 1992), practical applications do not require following the entire material separation process but only determining its initiation.

However, exploring the entire space of the design variables and finding the optimal design for each component can be time consuming. Therefore, model reduction procedures play a significant role in this context. Their capabilities are briefly described in the following.

2. GNT model

GNT plasticity model represents an extension of the classical Hencky-Huber-von Mises (HHM) formulation, where an additional variable field is introduced to represent the micro-porosity distribution, f. Thus, for instance, the yield function Φ can be formulated as:

$$\Phi = \left(\frac{q}{\sigma_y}\right)^2 + 2q_1 f cosh\left(-q_2 \frac{3p}{2\sigma_y}\right) - (1 + q_3 f^2) \tag{1}$$

where: p and q indicate the mean stress and the equivalent deviatoric stress in the classical von Mises' sense (see, e.g., Chen and Han, 1988); σ_y represents the yield limit; q_1, q_2 and q_3 are other material constants.

The initial porosity value is progressively increased by void nucleation and growth. These processes are controlled by the distribution of the plastic strains, and described by the rate expression:

$$\dot{f} = (1 - f)\dot{v}^p + \left(\frac{f_N}{S_N\sqrt{2\pi}}\, exp\left[-\frac{1}{2}\left(\frac{e^p - \varepsilon_N}{S_N}\right)^2\right]\right)\dot{e^p} \tag{2}$$

where $\dot{v}^p$ and $\dot{e^p}$ represent the volumetric and equivalent (in von Mises' sense) plastic strain rates, respectively, while f_N, ε_N and S_N are further model parameters. In particular, f_N modulates the nucleation rate of the new voids, while ε_N and S_N represent the mean value and the standard deviation of the (assumed Gaussian) distribution of the residual strains due to the production process.

The actual values of several constitutive properties entering relations (1) and (2) are usually difficult to be determined, either due to the lack of a direct mechanical meaning or due to their intrinsic origin. However, their knowledge is essential to reproduce the actual response and failure mode of the material. This is particularly true when the metal constitutes the matrix of a composite, where the damage distribution is also influenced by geometry details and imperfections, as shown for instance in Fig. 1. An extensive exploration of the design space is therefore required, either to structural optimization purposes and/or for parameter identification.

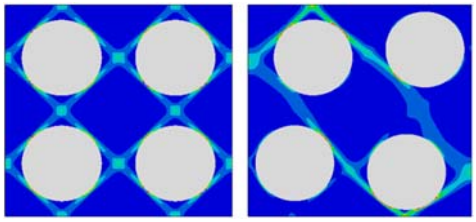

Fig. 1. Strain localization bands preceding material separation in the transversal plane of a long fiber composite, in the case of regular (left) or slightly scattered (right) distribution of the reinforcement in a representative volume element.

3. Surrogate analytical models

The computational burden associated to repetitive non-linear analyses can be greatly reduced by replacing the FE approach with analytical surrogates, which consist in the interpolation of the results obtained from a limited number of simulations performed for predetermined combinations of the parameter values (training set), tailoring the numerical efforts on the desired accuracy (Hernandez et al., 2014).

The analytical surrogates can be optimized by the selection of suitable interpolation functions. Radial basis functions (RBFs) are often employed in this context since they produce good approximation of highly non-linear mappings starting from a relatively low number of sampling points, freely defined in the assumed parameter space (Bolzon and Talassi, 2012). Their flexibility allows to improve the results sequentially and, possibly, to include the output of real experiments in the training set.

Accuracy can be further improved by filtering the noises associated with the initial numerical or experimental results by data compression schemes, for instance based on proper orthogonal decomposition (POD), see e.g. de Gooijer et al. (2021). This provision can filter out most disturbances, retaining the essential features of the system response.

A detailed explanation of these methodologies and their application to smooth problems is presented, for instance, in Bolzon and Bulijak (2011).

4. Representative results

The damaging processes developing in the metal-ceramic composites considered in this contribution are characterized by localized phenomena. For example, Fig. 2 shows the plastic strain distribution in the periodic cell of a fiber reinforced metal-matrix composite with 40% ceramic content under macroscopic uniaxial deformation in the transversal plane. The graphs display the output of FE analyses carried out for the parameter values defining the corner nodes of the (typical) parameter domain represented in Fig. 3(a), while the remaining materials characteristics are kept constant. The strain patterns are similar, but the magnitude differs case to case.

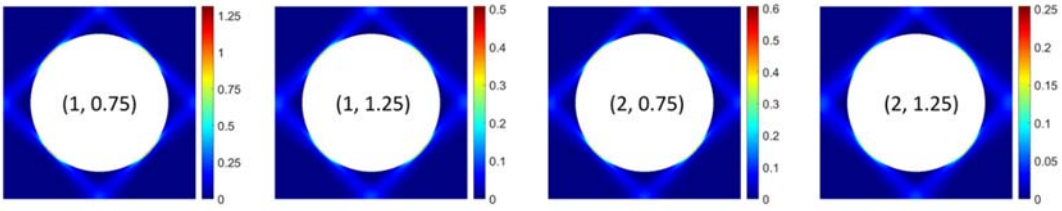

Fig. 2. Plastic strain distribution at the peak macroscopic stress in a unit periodic cell for the parameter values that define the corner nodes of the domain represented in Fig. 3(a); in parentheses, the (q_1, q_2) values corresponding to each graph.

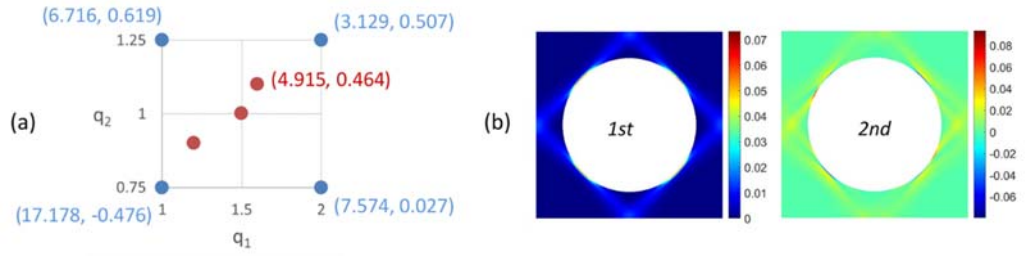

Fig. 3. (a) The considered sub-domain in the parameter space; (b) the first two main deformation modes recovered by POD from the plastic strain distributions represented in Fig. 2.

The same information contained in Fig. 2 can be represented alternatively, introducing small sets of factors that amplify the primary deformation modes, or bases, which can be recovered by POD analysis. The first two of them are visualized in Fig. 3(b). The number of bases to be considered depends on the desired detail level. However, higher modes are usually discarded since they mainly reflect numerical (or experimental) noises.

The blue digits in Fig. 3(a) represent the combination factors that allow to reconstruct the graphs in Fig. 2 as a combination of the modes displayed in Fig. 3(b). These coefficients can then be interpolated to obtain the plastic strain distribution in the whole parameter domain (see, e.g., the red digits corresponding to one internal point), with an accuracy comparable to that of the training set.

This approach possesses high sensitivity to the parameter values, also in situations that produce similar results. This is for instance the case of the microstructure with smaller (10%) ceramic content visualized in Fig. 4. In this case, the maximum equivalent strain value varies slightly, as indicated in Table 1, despite the large extension of the parameter space, which spans two orders of magnitude of the initial porosity value, f_0. Nonetheless, the different situations are clearly distinguished by the amplification factors that allow to reconstruct the residual strain field as combination of the bases shown in Fig. 4(b). Here, the contribution of the second deformation mode is particularly relevant in highlighting the role of parameter ε_N.

Table 1. Macroscopic strain at 4% macroscopic strain, microstructure in Fig. 4(b).

f_0	ε_n	Maximum equivalent plastic strain
0.0005	0.1	0.144
0.0005	4	0.139
0.05	0.1	0.134
0.05	4	0.130

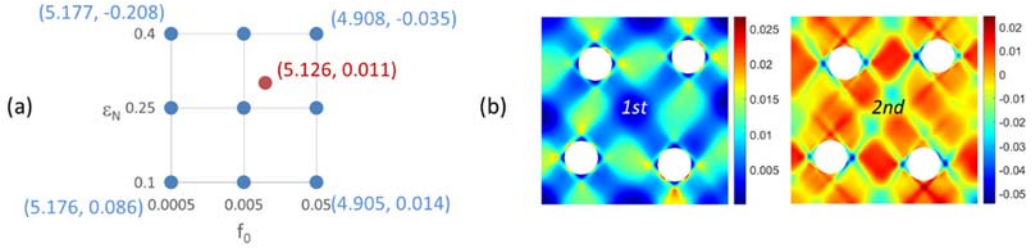

Fig. 4. (a) The considered sub-domain in the parameter space; (b) the first two main deformation modes.

5. Closing remarks

Surrogate analytical models based on POD reduction and RBF interpolation perform well even in the presence of localized phenomena. Based on these approaches, small sets of combination factors can effectively replace complex numerical analyses, exhibiting high sensitivity to the main problem variables. Large parameter spaces can then be explored in reasonable times to find optimal design solutions and/or identify material parameters not amenable to direct measurement.

References

Babout, L., Maire, E., Buffiere, J.-Y., Fougeres, R., 2001. Characterization by X-ray computed tomography of decohesion, porosity growth and coalescence in model metal matrix composites. Acta Materialia 49, 2055–2063.

Babout, L., Maire, E., Fougeres, R., 2004. Damage initiation in in model metallic materials: X-ray tomography and modelling. Acta Materialia 52, 2475–2487.

Bolzon, G., Buljak, V., 2011. An effective computational tool for parametric studies and identification problems in materials mechanics. Computational Mechanics 48, 675–687.

Bolzon, G., Pitchai, P., 2017. Applications and modelling challenges of metal matrix composites. In: Vieira, A.F.C. (Ed.). Material Modelling: Applications, Challenges and Research. Nova Science Publishers, New York, pp. 71–88.

Bolzon, G., Pitchai, P., 2022. The influence of imperfect interfaces on the measurable effective properties of ceramic composites. Composite Interfaces 29, 1013-1032.

Bolzon, G., Talassi, M., 2012. Model reduction techniques in computational materials mechanics. In: Zavarise, G., Boso, D.P. (Eds.). Bytes and Science, CIMNE, Barcelona, pp. 131–141.

Bonora, N., Ruggiero, A., 2006. Micromechanical modeling of composites with mechanical interface – Part II: Damage mechanics assessment. Composites Science and Technology 66, 323–332.

Chen, W.F., Han, D.J., 1988. Plasticity for Structural Engineers. Springer-Verlag, New York.

de Gooijer, B.M., Havinga, J., Geijselaers, H.J.M., van den Boogaard, A.H., 2021. Evaluation of POD based surrogate models of fields resulting from nonlinear FEM simulations. Advanced Modeling and Simulation in Engineering Science 8, 25.

Gurson, A.L., 1977. Continuum theory of ductile rupture by void nucleation and growth: Part I—Yield criteria and flow rules for porous ductile media. Journal of Engineering Materials and Technology 99, 2–15.

Hernández, J., Oliver, J., Huespe, A.E., Caicedo, M., Cante, J., 2014. High-performance model reduction techniques in computational multiscale homogenization. Computer Methods in Applied Mechanics and Engineering 276, 149–189.

Hild, F., Larsson, P.-L., Leckie, F.A., 1992. Localization due to damage in fiber-reinforced composites. International Journal of Solids and Structures 29, 3221–3238.

Needleman, A., Tvergaard, V., 1984. An analysis of ductile rupture in notched bars. Journal of the Mechanics and Physics of Solids 32, 461–490.

Palizvan, M., Abadi, M.T., Sadr, M.H., 2020. Micromechanical damage behavior of fiber-reinforced composites under transverse loading including fiber-matrix debonding and matrix cracks. International Journal of Fracture 226, 1–16.

Vaz, M. Jr, Muñoz-Rojas, P.A., Cardoso, E.L., Tomiyama, M., 2016. Considerations on parameter identification and material response for Gurson-type and Lemaitre-type constitutive models. International Journal of Mechanical Sciences 106, 254–265.